$RE_4B_4O_{11}F_2$ (RE = Pr, Nd): Two New Rare-earth Fluoride Borates Isotypic to $Gd_4B_4O_{11}F_2$

Matthias Glätzle and Hubert Huppertz

Institut für Allgemeine, Anorganische und Theoretische Chemie, Leopold-Franzens-Universität Innsbruck, Innrain 80 – 82, A-6020 Innsbruck, Austria

Reprint requests to H. Huppertz. E-mail: Hubert.Huppertz@uibk.ac.at

Z. Naturforsch. **2013**, *68b*, 635 – 642 / DOI: 10.5560/ZNB.2013-3086
Received February 27, 2013

Dedicated to Professor Heinrich Nöth on the occasion of his 85th birthday

The rare-earth fluoride borates $RE_4B_4O_{11}F_2$ (RE = Pr, Nd) were obtained in a Walker-type multianvil device from the corresponding rare-earth oxides and fluorides, and boron oxide. $Pr_4B_4O_{11}F_2$ was obtained under high-pressure/high-temperature conditions of 8.5 GPa/1150 °C, and $Nd_4B_4O_{11}F_2$ at 8 GPa and 1300 °C. The single-crystal structure determinations revealed that both compounds are isotypic to $RE_4B_4O_{11}F_2$ (RE = Eu, Gd, Dy), crystallizing in the space group $C2/c$ ($Z = 4$) with the parameters $a = 1397.3(3)$, $b = 472.78(9)$, $c = 1400.2(3)$ pm, $\beta = 91.1(1)°$, $V = 0.9248(3)$ nm^3, $R_1 = 0.0444$, and $wR_2 = 0.0539$ (all data) for $Pr_4B_4O_{11}F_2$, and $a = 1389.1(3)$, $b = 471.2(1)$, $c = 1394.4(3)$ pm, $\beta = 91.1(1)°$, $V = 0.9125(3)$ nm^3, $R_1 = 0.0286$, and $wR_2 = 0.0601$ (all data) for $Nd_4B_4O_{11}F_2$. The structure type of $Gd_4B_4O_{11}F_2$ contains BO_4 tetrahedra as well as BO_3 groups connected *via* common corners. Here, we report about the crystallographic characterization of both compounds in comparison to the isotypic phases and discuss their IR spectra.

Key words: Rare-Earth, Fluoride, Borate, High Pressure, Crystal Structure

Introduction

Borates have been the subject of intensive investigation during the past few decades. Due to their ability to form BO_3 groups as well as BO_4 tetrahedra, they exhibit a large structural diversity, possibly exceeding that of silicates. Presently, more than 1100 different crystal structures of borates are listed in the Inorganic Crystal Structure Database [1]. The development of sophisticated high-pressure synthetic methods has been the foundation of our work in the past 15 years, which has led to new high-pressure polymorphs of known (ambient-pressure) oxoborates, *e. g.* β-MB_4O_7 (M = Ca, Zn, Hg) and χ-$REBO_3$ (RE = Dy–Er). Besides that, we were also able to synthesize new compositions like $RE_3B_5O_{12}$ (RE = Sc, Er–Lu), $RE_4B_{10}O_{21}$ (RE = Pr), and $RE_4B_6O_{15}$ (RE = Dy, Ho), the latter showing for the first time the structural motif of edge-sharing BO_4 tetrahedra. In recent years, our research expanded the field towards fluorido borates and fluorido borates. These compounds, especially "fluoroborate" glasses doped with rare-earth elements, are well known for their interesting luminescence, fluorescence, and even dielectric properties. In contrast, less is known regarding crystalline fluorido borates and fluoride borates, except for naturally occurring minerals containing more than two cations. A summary of the achievements reached so far can be found in refs. [2] and [3].

For the chemical composition $RE_4B_4O_{11}F_2$, two different structure types were obtained by high-pressure/high-temperature syntheses. In 2010, Haberer *et al.* presented the compound $La_4B_4O_{11}F_2$ [4] crystallizing in space group $P2_1/c$ with the lattice parameters $a = 778.1(2)$, $b = 3573.3(7)$, $c = 765.7(2)$ pm, and $\beta = 113.92(3)°$ ($Z = 8$). The crystal structure consists of BO_3 groups (Δ) which are either isolated (Δ), connected *via* common corners ($\Delta\Delta$), or connected *via* BO_4 tetrahedra forming the fundamental building block (FBB) $2\Delta\square{:}\Delta\square\Delta$ (after Burns *et al.* [5]).

Earlier in 2010, Haberer *et al.* discovered the fluoride borate $Gd_4B_4O_{11}F_2$ [6] showing the same atomic composition $RE_4B_4O_{11}F_2$ but a completely different crystal structure in space group $C2/c$. It contains BO_3

groups and BO_4 tetrahedra connected *via* common corners. The structural motif consists of two BO_3 groups (Δ) and two BO_4 tetrahedra (□), and can be described with the fundamental building block 2Δ2□:Δ□□Δ, which represented a novelty in borate chemistry. Later in 2010, Haberer *et al.* were able to synthesize two compounds crystallizing isotypically to $Gd_4B_4O_{11}F_2$, namely $Eu_4B_4O_{11}F_2$ and $Dy_4B_4O_{11}F_2$ [7].

Here, we report about two new compounds $RE_4B_4O_{11}F_2$ (RE = Pr, Nd) in this system, which are isotypic to $RE_4B_4O_{11}F_2$ (RE = Eu, Gd, Dy) [6, 7]. The syntheses and crystal structures of $RE_4B_4O_{11}F_2$ (RE = Pr, Nd) are discussed in comparison to the isotypic compounds, and the IR spectra of both new compounds are presented.

Experimental Part

Syntheses

The syntheses of the rare-earth fluoride borates $RE_4B_4O_{11}F_2$ (RE = Pr, Nd) were achieved by the reactions of the oxides Pr_6O_{11} and Nd_2O_3 with the corresponding rare-earth fluorides REF_3 (RE = Pr, Nd) and B_2O_3 under high-pressure/high-temperature conditions according to the Eqs. 1 and 2.

$$5\,Pr_6O_{11} + 6\,PrF_3 + 18\,B_2O_3 \xrightarrow[1150\,^\circ C]{8.5\ GPa} 9\,Pr_4B_4O_{11}F_2 + 5\,O_2 \quad (1)$$

$$5\,Nd_2O_3 + 2\,NdF_3 + 6\,B_2O_3 \xrightarrow[1300\,^\circ C]{8.5\ GPa} 3\,Nd_4B_4O_{11}F_2 \quad (2)$$

Stoichiometric mixtures of Pr_6O_{11} (Strem Chemicals, 99.9 %) or Nd_2O_3 (Strem Chemicals, 99.9 %) with the corresponding rare-earth fluoride PrF_3 (Strem Chemicals, 99.9 %) or NdF_3 (Strem Chemicals, 99.9 %) and B_2O_3 (Strem Chemicals, 99.9+ %) were ground up in a glove box under inert gas atmosphere and filled into boron nitride crucibles (Henze Boron Nitride Products GmbH, HeBoSint® P100, Kempten/Germany). These crucibles were positioned in the center of 14/8 assemblies and compressed by eight tungsten carbide cubes (Hawedia, ha-7 %Co, Marklkofen/Germany). A detailed description of the assemblies and their preparation can be found in refs. [8 – 12]. Pressure was applied *via* a Walker-type multianvil device and a 1000 ton press (both devices from the company Voggenreiter, Mainleus/Germany). The synthesis of $Pr_4B_4O_{11}F_2$/$Nd_4B_4O_{11}F_2$ started by compressing the educt mixtures up to 8.5/8 GPa in about three hours, and keeping them at this pressure for the following heating period. The temperature was increased to 1150/1300 °C in 10 min. and kept there for 15/10 min. Afterwards, the temperature was lowered to 500 °C in 20/25 min and finally to room temperature by switching off the heating. The decompression of the assemblies took about nine hours. The recovered MgO octahedra (Ceramic Substrates & Components Ltd., Newport, Isle of Wight/UK) were broken apart, and the surrounding graphite and the boron nitride crucibles were carefully removed from

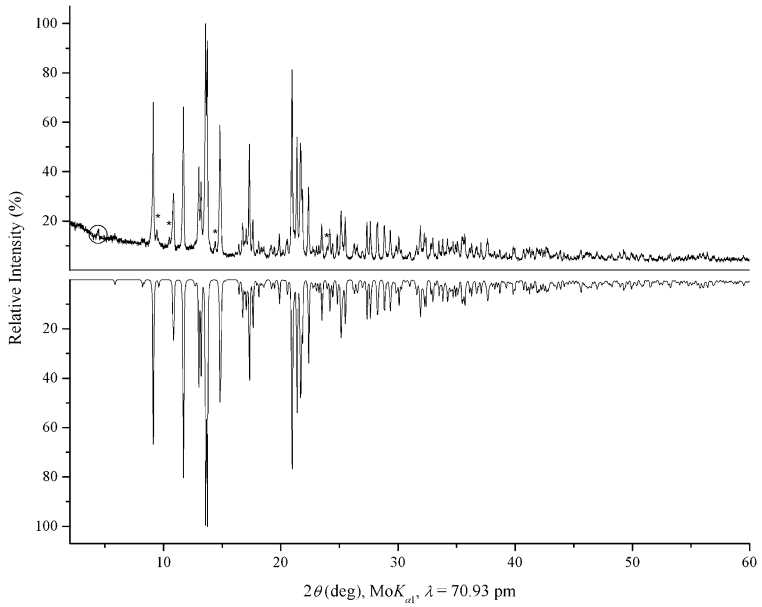

Fig. 1. Top: experimental powder pattern of $Nd_4B_4O_{11}F_2$; the reflections of γ-$Nd(BO_2)_3$ are indicated with asterisks, one unexplained reflection is marked with a circle. Bottom: theoretical powder pattern of $Nd_4B_4O_{11}F_2$, based on single-crystal diffraction data.

Table 1. Crystal data and structure refinement of $RE_4B_4O_{11}F_2$ (RE = Pr, Nd) (standard deviations in parentheses).

Empirical formula	$Pr_4B_4O_{11}F_2$	$Nd_4B_4O_{11}F_2$
M_r	820.88	834.20
Crystal system	monoclinic	
Space group	$C2/c$	
Powder diffractometer	Stoe Stadi P	
Radiation; λ, pm	Mo$K_{\alpha1}$; 70.93 (Ge(111) monochromator)	
Powder data		
a, pm	1396.7(5)	1388.4(4)
b, pm	472.7(2)	470.7(2)
c, pm	1400.0(3)	1392.8(5)
β, deg	91.1(1)	91.1(1)
V, nm^3	0.9242(3)	0.9100(3)
Single-crystal diffractometer	Nonius Kappa CCD	
Radiation; λ, pm	MoK_α; 71.073 (graphite monochromator)	
Single-crystal data		
a, pm	1397.3(3)	1389.1(3)
b, pm	472.78(9)	471.2(1)
c, pm	1400.2(3)	1394.4(3)
β, deg	91.1(1)	91.1(1)
V, nm^3	0.9248(3)	0.9125(3)
Formula units per cell	$Z = 4$	
Calculated density, g cm^{-3}	5.90	6.07
Crystal size, mm^3	$0.035 \times 0.025 \times 0.015$	$0.04 \times 0.02 \times 0.02$
Temperature, K	293(2)	293(2)
Absorption coefficient, mm^{-1}	20.8	22.5
F(000), e	1448	1464
θ range, deg	2.9–37.9	2.9–37.8
Range in hkl	$-24/+23$, $-8/+7$, $-24/+21$	±23, ±8, ±24
Total no. of reflections	7644	8055
Independent reflections / R_{int}	2464 / 0.0426	2442 / 0.0455
Reflections with $I > 2\sigma(I)$ / R_σ	1986 / 0.0448	2209 / 0.0373
Data / ref. parameters	2464 / 97	2442 / 97
Absorption correction	multi-scan (SCALEPACK [14])	
Goodness-of-fit on F^2	1.075	1.052
Final indices R_1 / wR_2 [$I > 2\sigma(I)$]	0.0299 / 0.0502	0.0249 / 0.0583
Indices R_1 / wR_2 (all data)	0.0444 / 0.0539	0.0286 / 0.0601
Largest diff. peak/hole, $\times 10^{-6}$ e pm^{-3}	2.4 / –2.7	2.5 / –2.2

the samples. $Pr_4B_4O_{11}F_2$ and $Nd_4B_4O_{11}F_2$ were obtained as green/purple air- and water-resistant crystals.

Crystal structure analyses

$Pr_4B_4O_{11}F_2$ and $Nd_4B_4O_{11}F_2$ were identified by powder X-ray diffraction in transmission geometry from plane samples of the reaction products, using a Stoe Stadi P powder diffractometer with Ge(111)-monochromatized Mo$K_{\alpha1}$ radiation (λ = 70.93 pm). Fig. 1 shows the powder pattern of $Nd_4B_4O_{11}F_2$ with some weak reflections of the byproduct γ-$Nd(BO_2)_3$ [13] (marked with asterisks). The experimental powder pattern (top) is in good agreement with the theoretical pattern (bottom) simulated from the single-crystal data. By indexing the reflections of the praseodymium fluoride borate, the parameters $a = 1396.7(5)$, $b = 472.7(2)$, $c = 1400.0(3)$ pm, $\beta = 91.1(1)^\circ$, and a volume of 0.9242(3) nm^3 were obtained. The indexing of the corresponding neodymium fluoride borate powder diffraction pattern led to the parameters $a = 1388.4(4)$, $b = 470.7(2)$, $c = 1392.8(5)$ pm, $\beta = 91.1(1)^\circ$, and a volume of 0.9100(3) nm^3. These validated the lattice parameters received from the single-crystal X-ray diffraction data for $Pr_4B_4O_{11}F_2$ and $Nd_4B_4O_{11}F_2$ (Table 1).

For the single-crystal structure analyses, small trapezoid platelets of both $Pr_4B_4O_{11}F_2$ and $Nd_4B_4O_{11}F_2$ were isolated by mechanical fragmentation. The intensity data of the single-crystals were collected at room temperature with a Kappa CCD diffractometer (Bruker AXS/Nonius, Karlsruhe) equipped with a Miracol fiber optics collimator and a Nonius FR590 generator (graphite-monochromatized MoK_α radiation, λ = 71.073 pm). Semiempirical absorption corrections based on multi-scans were performed with the program SCALEPACK [14]. The positional parameters of the isotypic compound $Gd_4B_4O_{11}F_2$ were used as starting values [6]. The parameter refinements (full-matrix least-squares

Table 2. Atomic coordinates and isotropic equivalent displacement parameters (U_{eq} in Å^2) for $RE_4B_4O_{11}F_2$ (RE = Pr, Nd) (space group: $C2/c$) (standard deviations in parentheses). U_{eq} is defined as one third of the trace of the orthogonalized U_{ij} tensor.

Atom	Wyckoff position	x	y	z	U_{eq}
Pr1	8f	0.05876(2)	0.52333(4)	0.37081(2)	0.00590(6)
Pr2	8f	0.27884(2)	0.02056(4)	0.37149(2)	0.00612(6)
B1	8f	0.9073(3)	0.9801(8)	0.2849(3)	0.0069(7)
B2	8f	0.0942(3)	0.9519(9)	0.5275(3)	0.0085(7)
O1	8f	0.9125(2)	0.8740(5)	0.3921(2)	0.0070(5)
O2	8f	0.1703(2)	0.8191(6)	0.2576(2)	0.0083(5)
O3	8f	0.0791(2)	0.6634(5)	0.5367(2)	0.0078(5)
O4	4e	0	0.8563(8)	1/4	0.0065(6)
O5	8f	0.1126(2)	0.0586(6)	0.4382(2)	0.0103(5)
O6	8f	0.9001(2)	0.2787(5)	0.2739(2)	0.0090(5)
F1	8f	0.2305(2)	0.5240(5)	0.4255(2)	0.0126(5)
Nd1	8f	0.05836(2)	0.52277(3)	0.37077(2)	0.00563(5)
Nd2	8f	0.27902(2)	0.02088(3)	0.37156(2)	0.00592(5)
B1	8f	0.9074(3)	0.9802(6)	0.2850(2)	0.0058(5)
B2	8f	0.0945(2)	0.9530(7)	0.5266(2)	0.0064(5)
O1	8f	0.9125(2)	0.8744(4)	0.3928(2)	0.0054(3)
O2	8f	0.1714(2)	0.8178(4)	0.2575(2)	0.0077(3)
O3	8f	0.0797(2)	0.6658(4)	0.5361(2)	0.0074(3)
O4	4e	0	0.8558(6)	1/4	0.0052(4)
O5	8f	0.1130(2)	0.0590(5)	0.4376(2)	0.0087(4)
O6	8f	0.9003(2)	0.2794(4)	0.2747(2)	0.0085(3)
F1	8f	0.2306(2)	0.5236(4)	0.4244(2)	0.0134(4)

against F^2) were achieved by using the SHELXS/L-97 software suite [15, 16]. All atoms were refined with anisotropic displacement parameters. Final difference Fourier syntheses did not reveal any significant residual peaks. All relevant details of the data collections and evaluations are given in Table 1. The positional parameters, interatomic distances, and interatomic angles are listed in the Tables 2 – 4.

Further details of the crystal structure investigations may be obtained from the Fachinformationszentrum Karlsruhe, 76344 Eggenstein-Leopoldshafen, Germany (fax: +49-7247-808-666; e-mail: crysdata@fiz-karlsruhe.de, http://www.fiz-informationsdienste.de/en/DB/icsd/depot_anforderung.html) on quoting the deposition numbers CSD-425572 and CSD-425573 for $Pr_4B_4O_{11}F_2$ and $Nd_4B_4O_{11}F_2$, respectively.

Vibrational spectroscopy

The ATR-FT-IR spectra of $Pr_4B_4O_{11}F_2$ and $Nd_4B_4O_{11}F_2$ were measured from small amounts of the grinded products utilizing a Bruker ALPHA-P "Platinum-ATR" FT-IR spectrometer with a spectral resolution of less than 2 cm^{-1}. The IR radiation with a wavelength of 850 nm was produced by a HeNe laser, and the reflected beam was detected by a DTGS detector at room temperature. For the measurements, the samples were positioned between two small diamond crystals of the IR spectrometer. 360 scans of each sample and the background were acquired using the OPUS 7.0 [17] software.

Results and Discussion

As reported for the isotypic phases $RE_4B_4O_{11}F_2$ (RE = Eu, Gd, Dy) [6, 7], the new compounds $RE_4B_4O_{11}F_2$ (RE = Pr, Nd) also form in a wide pressure and temperature range. In many syntheses with varying pressure and temperature conditions, the desired phases $RE_4B_4O_{11}F_2$ (RE = Pr, Nd) were the main products, but contained small amounts of the corresponding high-pressure rare-earth metaborates γ-$RE(BO_2)_3$ (RE = Pr, Nd) [13]. $Pr_4B_4O_{11}F_2$ could be obtained under pressure conditions reaching from 5.5 to 10.5 GPa and temperatures from 850 to 1150 °C. $Nd_4B_4O_{11}F_2$ was the main product arising at reaction conditions of 8 to 11.5 GPa and 1150 to 1300 °C. Obviously, this composition and the associated $Gd_4B_4O_{11}F_2$ structure type seem to have a remarkable tendency towards formation under these extreme conditions for both small and large rare-earth cations. Up to now, only $La_4B_4O_{11}F_2$ as a stoichiometrically identical but structurally completely different rare-earth fluoride borate is known. It crystallizes in a different structure type in the space group $P2_1/c$.

The synthesis of "$Ce_4B_4O_{11}F_2$" as the missing link between $La_4B_4O_{11}F_2$ and $Pr_4B_4O_{11}F_2$ has been attempted several times in our group using various reaction conditions, but without any success. The products

Table 3. Interatomic distances (pm) in $RE_4B_4O_{11}F_2$ (RE = Pr, Nd) (space group: $C2/c$), calculated with the single-crystal lattice parameters (standard deviations in parentheses).

Pr1–O6a	241.1(3)	Pr2–O2a	237.9(3)	B1–O6	142.3(5)
Pr1–O3a	242.6(3)	Pr2–O2b	241.0(3)	B1–O2	144.4(5)
Pr1–O4	244.2(2)	Pr2–O6	247.7(3)	B1–O4	151.1(4)
Pr1–O5a	250.2(3)	Pr2–O3	250.1(3)	B1–O1	158.3(5)
Pr1–F1	250.6(3)	Pr2–O1	251.9(3)		∅ = 149.0
Pr1–O3b	250.3(3)	Pr2–O5	252.6(3)		
Pr1–O2	264.5(3)	Pr2–F1a	256.1(2)	B2–O5	137.7(5)
Pr1–O1	265.3(3)	Pr2–F1b	259.1(2)	B2–O3	138.6(5)
Pr1–O5b	279.9(3)	Pr2–F1c	285.5(3)	B2–O1	139.9(5)
Pr1–O6b	282.5(3)		∅ = 253.5		∅ = 138.7
	∅ = 257.1				
F1–Pr1	250.6(3)				
F1–Pr2a	256.1(2)				
F1–Pr2b	259.1(2)				
F1–Pr2c	285.5(3)				
	∅ = 262.8				
Nd1–O6a	240.9(2)	Nd2–O2a	236.4(2)	B1–O6	142.1(4)
Nd1–O3a	241.5(2)	Nd2–O2b	239.2(2)	B1–O2	145.2(4)
Nd1–O4	243.0(2)	Nd2–O6	245.9(2)	B1–O4	150.3(3)
Nd1–O5a	248.8(2)	Nd2–O3	248.8(2)	B1–O1	158.5(4)
Nd1–F1	249.3(2)	Nd2–O5	250.6(2)		∅ = 149.0
Nd1–O3b	249.9(2)	Nd2–O1	250.6(2)		
Nd1–O1	264.0(2)	Nd2–F1a	255.0(2)	B2–O5	136.6(4)
Nd1–O2	264.3(2)	Nd2–F1b	257.4(2)	B2–O3	137.5(4)
Nd1–O5b	279.3(2)	Nd2–F1c	285.9(2)	B2–O1	139.2(4)
Nd1–O6b	279.6(2)		∅ = 252.2		∅ = 137.8
	∅ = 256.1				
F1–Nd1	249.3(2)				
F1–Nd2a	255.0(2)				
F1–Nd2b	257.4(2)				
F1–Nd2c	285.9(2)				
	∅ = 261.9				

Table 4. Interatomic angles (deg) in $RE_4B_4O_{11}F_2$ (RE = Pr, Nd) (space group: $C2/c$), calculated with the single-crystal lattice parameters (standard deviations in parentheses).

O6–B1–O2	115.3(3)	O5–B2–O3	118.4(3)	Pr1–F1–Pr2a	99.6(1)
O6–B1–O4	114.1(3)	O5–B2–O1	122.1(3)	Pr1–F1–Pr2b	99.4(1)
O2–B1–O4	107.7(3)	O3–B2–O1	119.5(3)	Pr1–F1–Pr2c	104.0(1)
O6–B1–O1	114.8(3)		∅ = 120.0	Pr2a–F1–Pr2b	133.2(1)
O2–B1–O1	104.1(3)			Pr2a–F1–Pr2c	112.3(1)
O4–B1–O1	99.2(3)			Pr2b–F1–Pr2c	103.9(1)
	∅ = 109.2				∅ = 108.7
O6–B1–O2	115.5(3)	O5–B2–O3	118.6(3)	Nd1–F1–Nd2a	99.9(1)
O6–B1–O4	114.4(3)	O5–B2–O1	122.4(3)	Nd1–F1–Nd2b	99.6(1)
O2–B1–O4	107.8(2)	O3–B2–O1	118.9(2)	Nd1–F1–Nd2c	103.6(1)
O6–B1–O1	114.2(2)		∅ = 120.0	Nd2a–F1–Nd2b	133.7(1)
O2–B1–O1	104.0(2)			Nd2a–F1–Nd2c	111.9(1)
O4–B1–O1	99.3(2)			Nd2b–F1–Nd2c	103.6(1)
	∅ = 109.2				∅ = 108.7

of the reactions were γ-$Ce(BO_2)_3$ and a not yet identified phase. Apparently, the cerium cation has an exceptionally low tendency to form fluoride borates. To the best of our knowledge, no cerium fluoride borate is known up to now.

As depicted in Fig. 2, the structure of $RE_4B_4O_{11}F_2$ (RE = Pr, Nd) contains BO_3 groups and BO_4 tetrahedra connected *via* common corners. Two BO_3 groups (Δ) and two BO_4 tetrahedra ($\square$) build up the main structural motif, including a twofold rotation axis as a symmetry element. The structure has first been discovered in the phase $Gd_4B_4O_{11}F_2$ and can be described with the fundamental building block $2\Delta2\square$: $\Delta\square\square\Delta$. A detailed depiction of the crystal structure of

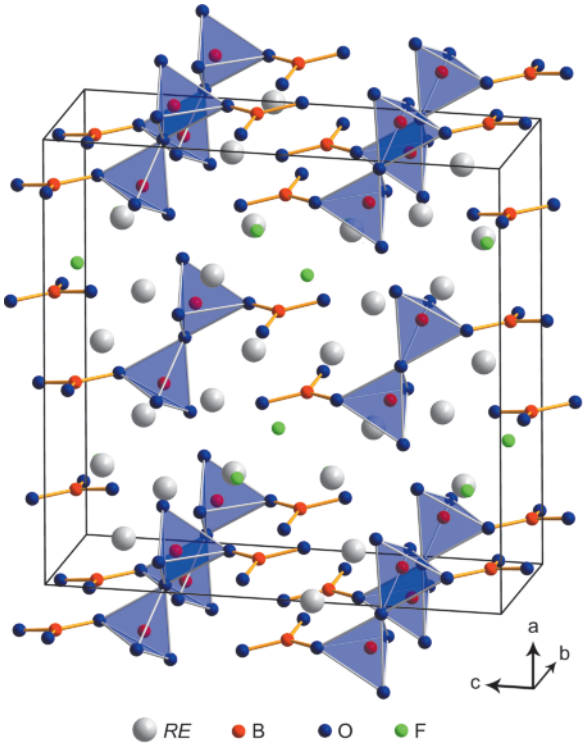

Fig. 2 (color online). Crystal structure of $RE_4B_4O_{11}F_2$ (RE = Pr, Nd) showing the fundamental building block 2Δ2□:Δ□□Δ.

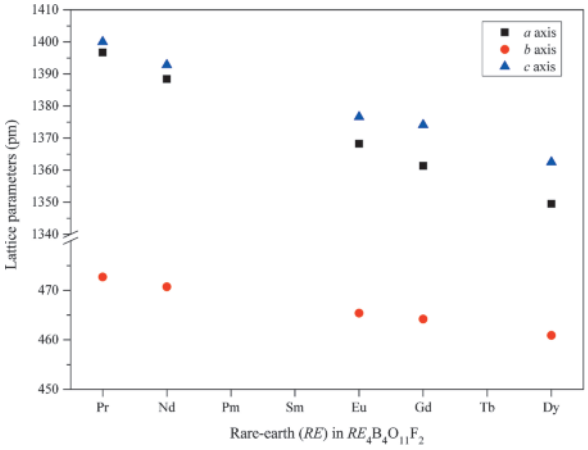

Fig. 3 (color online). Visualization of the progression of the lattice parameters (pm) of $RE_4B_4O_{11}F_2$ (RE = Pr, Nd, Eu, Gd, Dy) with the typical decrease due to the lanthanoid contraction.

$RE_4B_4O_{11}F_2$ (RE = Pr, Nd) can be found in the description of the isotypic compound $Gd_4B_4O_{11}F_2$ [6]. This paper gives a comparison of the five isotypic compounds $RE_4B_4O_{11}F_2$ (RE = Pr, Nd, Eu, Gd, Dy).

Fig. 3 shows a comparison of the lattice parameters of $Pr_4B_4O_{11}F_2$, $Nd_4B_4O_{11}F_2$, $Eu_4B_4O_{11}F_2$ [7], $Gd_4B_4O_{11}F_2$ [6], and $Dy_4B_4O_{11}F_2$ [7]. The exact values are given in Table 5. The variation of the lattice parameters corresponds to the decreasing ionic radii (lanthanoid contraction) of the rare-earth cations. The values for the ionic radii of ninefold coordinated cations are as follows: Pr^{3+} (131.9 pm), Nd^{3+} (130.3 pm), Eu^{3+} (126.0 pm), Gd^{3+} (124.7 pm), and Dy^{3+} (122.3 pm) [18]. Since the size differences are not too large, the bond lengths and angles of $RE_4B_4O_{11}F_2$ (RE = Pr, Nd) are comparable to the values found in the other isotypic compounds [6, 7]. In $Pr_4B_4O_{11}F_2$, the Pr–O/F distances are within 237.9(3) – 285.5(3) pm and in $Nd_4B_4O_{11}F_2$, the Nd–O/F distances are in the range 236.4(2) – 285.9(2) pm. Compared to the values of 230.0(3) – 283.7(3) pm for Gd–O/F in $Gd_4B_4O_{11}F_2$, the bond lengths in $Pr_4B_4O_{11}F_2$ and $Nd_4B_4O_{11}F_2$ are slightly but significantly shorter, just as expected. The crystal structure of $RE_4B_4O_{11}F_2$ (RE = Pr, Nd, Eu, Gd, Dy) contains a distorted tetrahedron that was interpreted as a BO_3 group, in which the boron atom is drawn towards a fourth oxygen atom, resulting in a long B–O bond [6]. This long B1–O1 bond measures 157.3(5) pm in $Eu_4B_4O_{11}F_2$, 159.0(6) pm in $Gd_4B_4O_{11}F_2$, and 156.6(8) pm in $Dy_4B_4O_{11}F_2$. The corresponding B–O distances in $Pr_4B_4O_{11}F_2$ and $Nd_4B_4O_{11}F_2$ are nearly identical with values of 158.3(5) and 158.5(4) pm, respectively. Obviously, the changing ionic radii of the rare-earth cations have no influence on the B1–O1 bond length. The BO_3 groups in $RE_4B_4O_{11}F_2$ (RE = Pr, Nd) have average B–O distances of 138.7 and 137.8 pm, respec-

Compound	a	b	c	β	V
$Pr_4B_4O_{11}F_2$	1396.7(5)	472.7(2)	1400.0(3)	91.1(1)	0.9242(3)
$Nd_4B_4O_{11}F_2$	1388.4(4)	470.7(2)	1392.8(5)	91.1(1)	0.9100(3)
$Eu_4B_4O_{11}F_2$	1368.2(3)	465.4(1)	1376.6(3)	91.2(1)	0.8765(3)
$Gd_4B_4O_{11}F_2$	1361.3(3)	464.2(2)	1374.1(3)	91.3(1)	0.8681(3)
$Dy_4B_4O_{11}F_2$	1349.5(3)	460.9(1)	1362.5(3)	91.3(1)	0.8472(3)

Table 5. Comparison of the single-crystal lattice parameters (pm, deg) and volumes (nm^3) of $RE_4B_4O_{11}F_2$ (RE = Pr, Nd, Eu, Gd, Dy) (standard deviations in parentheses).

Table 6. Charge distribution in $RE_4B_4O_{11}F_2$ (RE = Pr, Nd), calculated according to the BLBS (ΣV) [20 – 24] and CHARDI concepts (ΣQ) [22, 23, 25].

	Pr1	Pr2	B1	B2	Nd1	Nd2	B1	B2
ΣV	3.04	3.02	2.94	2.87	3.13	3.00	2.94	2.95
ΣQ	2.98	2.99	3.00	3.03	2.98	3.01	2.99	3.03
	O1	O2	O3	O4	O1	O2	O3	O4
ΣV	–2.09	–2.07	–2.16	–2.24	–2.10	–2.03	–2.16	–2.26
ΣQ	–1.99	–2.04	–2.12	–2.15	–1.97	–2.01	–2.12	–2.20
	O5	O6	F1		O5	O6	F1	
ΣV	–1.87	–1.89	–0.82		–1.89	–1.88	–0.82	
ΣQ	–1.87	–1.89	–1.03		–1.88	–1.90	–1.02	

tively – in perfect agreement with the literature value of 137.0 pm [19].

We calculated the bond valence sums of all atoms in $RE_4B_4O_{11}F_2$ (RE = Pr, Nd) according to the BLBS (bond length / bond strength, ΣV) [20 – 24] and CHARDI (*char*ge *di*stribution in solids) concepts (ΣQ) [22, 23, 25]. The results of both calculations have verified the formal valence states in the fluoride borates. Table 6 shows the formal ionic charges received from the calculations, which correspond to the expected values.

Furthermore, we calculated the MAPLE values (*Ma*delung *P*art of *L*attice *E*nergy) [26 – 28] of $RE_4B_4O_{11}F_2$ (RE = Pr, Nd) and compared them with the values for the binary components. We obtained 71 630 kJ mol^{-1} for $Pr_4B_4O_{11}F_2$, to be compared with 71 600 kJ mol^{-1} (deviation: 0.04 %) starting from the binary components [5/3 × Pr_2O_3 ([29], 14 474 kJ mol^{-1}) + 2 × B_2O_3-II ([30], 21 938 kJ mol^{-1}) + 2/3 × PrF_3 ([31], 5444 kJ mol^{-1})]. For $Nd_4B_4O_{11}F_2$, the resulting value is 71 766 kJ mol^{-1} compared to 71 946 kJ mol^{-1} (deviation: 0.25 %) based on the binary components [5/3 × Nd_2O_3 ([32], 14 564 kJ mol^{-1}) + 2 × B_2O_3-II ([30], 21 938 kJ mol^{-1}) + 2/3 × NdF_3 ([33], 5424 kJ mol^{-1})].

FT-IR spectroscopy

Fig. 4 shows the absorption bands of $Pr_4B_4O_{11}F_2$ and $Nd_4B_4O_{11}F_2$, which are typical for borates exhibiting BO_4 tetrahedra and BO_3 groups [34, 35]. In the range from 400 to 1600 cm^{-1}, three groups of bands can be distinguished: bands around 700 cm^{-1} typically arise from in-plane and out-of-plane bending vibrations of BO_3 groups, but can also be taken as an indication for both three- and four-fould coordinated boron atoms [6, 34 – 36]. The strong bands in the range of 900 – 1100 cm^{-1} can be assigned to stretching vibrations of tetrahedrally coordinated boron atoms [35, 37]. Between 1200 and 1500 cm^{-1}, absorption bands arise from stretching vibrations of trigonal borate groups [37, 38]. The FT-IR spectra of $Pr_4B_4O_{11}F_2$ and $Nd_4B_4O_{11}F_2$ clearly show the existence of both BO_4 tetrahedra and BO_3 groups in the crystal structure. Above 1600 cm^{-1}, no further absorp-

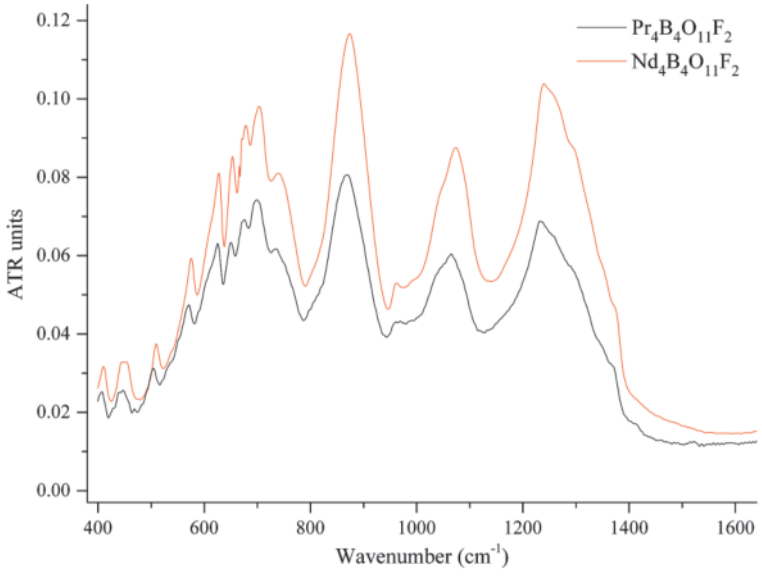

Fig. 4 (color online). ATR-FT-IR spectra of $Pr_4B_4O_{11}F_2$ (bottom curve) and $Nd_4B_4O_{11}F_2$ (top curve).

tion bands could be detected, leading to the conclusion that no substitution of fluoride or oxo anions by hydroxide groups has taken place.

Conclusion

With the syntheses of $RE_4B_4O_{11}F_2$ (RE = Pr, Nd), the number of compounds with the composition $RE_4B_4O_{11}F_2$ has been extended to five. While the existence of the compound "$Ce_4B_4O_{11}F_2$" could not be proven yet, it is very likely for the isotypic compounds $Sm_4B_4O_{11}F_2$ and $Tb_4B_4O_{11}F_2$; further studies on these phases and the possible formation of $RE_4B_4O_{11}F_2$ with RE = Ho–Lu are planned.

Acknowledgement

We would like to thank Dr. G. Heymann for collecting the single-crystal data. The research was funded by the Austrian Science Fund (FWF): P 23212-N19.

[1] *Inorganic Crystal Structure Data Base – ICSD*, Fachinformationszentrum (FIZ) Karlsruhe, Karlsruhe, **2013**; http://icsd.fiz-karlsruhe.de (accessed February 27, 2013).
[2] H. Huppertz, *Chem. Commun.* **2011**, *47*, 131.
[3] A. Pitscheider, Dissertation, Universität Innsbruck, Innsbruck **2011**.
[4] A. Haberer, R. Kaindl, O. Oeckler, H. Huppertz, *J. Solid State Chem.* **2010**, *183*, 1970.
[5] P. C. Burns, J. D. Grice, F. C. Hawthorne, *Can. Mineral.* **1995**, *33*, 1131.
[6] A. Haberer, R. Kaindl, H. Huppertz, *J. Solid State Chem.* **2010**, *183*, 471.
[7] A. Pitscheider, M. Enders, H. Huppertz, *Z. Naturforsch.* **2010**, *65b*, 1439.
[8] D. Walker, M. A. Carpenter, C. M. Hitch, *Am. Mineral.* **1990**, *75*, 1020.
[9] D. Walker, *Am. Mineral.* **1991**, *76*, 1092.
[10] H. Huppertz, *Z. Kristallogr.* **2004**, *219*, 330.
[11] D. C. Rubie, *Phase Transitions* **1999**, *68*, 431.
[12] N. Kawai, S. Endo, *Rev. Sci. Instrum.* **1970**, *8*, 1178.
[13] H. Emme, Ch. Despotopoulou, H. Huppertz, *Z. Anorg. Allg. Chem.* **2004**, *630*, 2450.
[14] Z. Otwinowski, W. Minor in *Methods in Enzymology*, Vol. 276, *Macromolecular Crystallography*, Part A (Eds.: C. W. Carter Jr, R. M. Sweet), Academic Press, New York, **1997**, pp. 307.
[15] G. M. Sheldrick, SHELXS/L-97, Programs for Crystal Structure Determination, University of Göttingen, Göttingen (Germany) **1997**.
[16] G. M. Sheldrick, *Acta Crystallogr.* **2008**, *A64*, 112.
[17] OPUS (version 7.0), Bruker Optik GmbH, Ettlingen (Deutschland) **2011**.
[18] R. D. Shannon, *Acta Crystallogr.* **1976**, *A32*, 751.
[19] E. Zobetz, *Z. Kristallogr.* **1982**, *160*, 81.
[20] L. Pauling, *J. Am. Chem. Soc.* **1947**, *69*, 542.
[21] A. Byström, K.-A. Wilhelmi, *Acta Chem. Scand.* **1951**, *5*, 1003.
[22] I. D. Brown, D. Altermatt, *Acta Crystallogr.* **1985**, *B41*, 244.
[23] N. E. Brese, M. O'Keeffe, *Acta Crystallogr.* **1991**, *B47*, 192.
[24] N. E. Brese, M. O'Keeffe, *Structure and Bonding*, Springer-Verlag, Berlin, **1989**.
[25] R. Hoppe, S. Voigt, H. Glaum, J. Kissel, H. P. Müller, K. J. Bernet, *J. Less-Common Met.* **1989**, *156*, 105.
[26] R. Hoppe, *Angew. Chem., Int. Ed. Engl.* **1966**, *5*, 96.
[27] R. Hoppe, *Angew. Chem., Int. Ed. Engl.* **1970**, *9*, 25.
[28] R. Hübenthal, M. Serafin, R. Hoppe, MAPLE (version 4.0), Program for the Calculation of Distances, Angles, Effective Coordination Numbers, Coordination Spheres, and Lattice Energies, University of Gießen, Gießen (Germany) **1993**.
[29] L. Eyring, N. C. Baenziger, *J. Appl. Phys.* **1962**, *33*, 428.
[30] C. T. Prewitt, R. D. Shannon, *Acta Crystallogr.* **1968**, *B24*, 869.
[31] O. Greis, R. Ziel, B. Breidenstein, A. Haase, T. Petzel, *Powder Diffr.* **1995**, *10*, 44.
[32] S. V. Chavan, M. D. Mathews, A. K. Tyagi, *Mater. Res. Bull.* **2005**, *40*, 1558.
[33] A. K. Tyagi, S. J. Patwe, S. N. Achary, M. B. Mallia, *J. Solid State Chem.* **2004**, *177*, 1746.
[34] G. Heymann, K. Beyer, H. Huppertz, *Z. Naturforsch.* **2004**, *59b*, 1200.
[35] J. P. Laperches, P. Tarte, *Spectrochim. Acta* **1966**, *22*, 1201.
[36] C. E. Weir, R. A. Schroeder, *J. Res. Natl. Bur. Stand.* **1964**, *68a*, 465.
[37] M. Ren, J. H. Lin, Y. Dang, L. Q. Yang, M. Z. Su, L. P. You, *Chem. Mater.* **1999**, *11*, 1576.
[38] W. C. Steele, J. C. Decius, *J. Chem. Phys.* **1956**, *25*, 1184.